Many-Body Entanglement in Short-Range Interacting Fermi Gases for Metrology

Leonardo Lucchesi[1] and Maria Luisa Chiofalo[1,2,3,*]
[1]Dipartimento di Fisica "Enrico Fermi" and INFN, Università di Pisa, Largo B. Pontecorvo 3, I-56127 Pisa, Italy
[2]JILA, University of Colorado, 440 UCB, Boulder, Colorado 80309, USA
[3]Kavli Institute for Theoretical Physics, University of California, Santa Barbara, CA 93106-4030, USA

(Received 21 February 2019; revised manuscript received 20 June 2019; published 9 August 2019)

We explore many-body entanglement in spinful Fermi gases with short-range interactions, for metrology purposes. We characterize the emerging quantum phases via density-matrix renormalization group simulations and quantify their entanglement content for metrological usability via quantum Fisher information (QFI). Our study establishes a method, promoting QFI to be an order parameter. Short-range interactions reveal to build up metrologically promising entanglement in the XY-ferromagnetic and cluster ordering, the cluster physics being unexplored so far.

DOI: 10.1103/PhysRevLett.123.060406

Strongly correlated systems are progressively becoming a paradigm for precision metrology, attracting broad interest [1]. Quantum gases represent a powerful platform to develop quantum measurement devices [2,3], bridging between engineering of quantum states of matter [4] and progress in atom interferometry [5,6]. Atom interferometry has many sources of uncertainty, classifiable into device and statistics-driven causes [7]. Accurate experimental schemes have blossomed, providing significant reduction of the former, now comparable or even lower than statistical error [7–12]. Further precision improvements can be obtained by addressing the statistical uncertainty problem, in particular the quantum phase estimation [13,14]. A conceptual tool to reduce statistical uncertainty may come from entanglement, specifically quantum squeezing [15–18], where uncertainty in a selected observable can be reduced below the Heisenberg bound at expenses of a conjugate observable [19]. Atomic spin squeezing has been implemented in numerous experimental setups, using interactions either collision driven or light mediated in optical cavities [15,20–23]. Entanglement is a necessary but not sufficient condition for squeezing, its metrological usefulness being quantified via quantum Fisher information (QFI) from the Cramér-Rao bound for statistical estimation of variances [1,14,24]. Generation of useful entanglement is often performed by means of infinite-range interactions [15,25,26], and can survive a power-law decay of the coupling [27]. However, also many-body finite-range interactions can drive long-range correlations, reinforcing the need to account for particles' indistinguishability [28] and making the quantification of entanglement an even more subtle issue, as witnessed by a timely debate [29–32] in both quantum information and many-body communities, also motivated by experimental observations in quantum gases [33]. The interesting question thus arises, whether short-range interactions can provide phases with useful entanglement content for metrology.

In this Letter, we tackle the problem from a conceptual perspective and investigate many-body entanglement via a minimal model able to reproduce the essential desirable features of a strongly correlated quantum fluid with short-range interactions and motional degrees of freedom [34]. To this aim, we consider a system of N fermionic atoms in two spin states within the tUJ model [35], correlated via nearest-neighbor coupling J and on-site U, and in the presence of tunneling processes t. We use density-matrix renormalization group (DMRG) simulations to characterize the system quantum phases and classify them by finding a quantitative correspondence between QFI and the order parameters characterizing the quantum fluid, conveying two central messages. First, this idea acquires methodological significance, since QFI can be seen as an order parameter. Second, two particular ground states in a short-range interacting system result especially promising for metrological use, because of their QFI scaling with the number of atoms N. These phases correspond to an XY ferromagnet and a cluster ordering, the latter being here identified and quantitatively analyzed in the whole U-J phase diagram. Exploiting this metrological usability requires the devising of suited protocols [36], which we will discuss along with possible experimental realizations.

The Fermionic tUJ model.—We consider an ensemble of fermions in two (real or pseudo)-spin states, moving in a one-dimensional (1D) geometry in the presence of a short-range interaction. We model the system as cartooned in Fig. 1 (top), according to the tUJ Hamiltonian:

$$H=\sum_i[-t(c^\dagger_{i\sigma}c_{i+1\sigma}+\text{H.c.})+Un_{i\uparrow}n_{i\downarrow}+J(s^+_i s^-_{i+1}+\text{H.c.})]. \tag{1}$$

Here, $c^{(\dagger)}_{j,\sigma}$ are destruction (creation) operators for fermions with spin σ on site j, $n_j\equiv\sum_\sigma c^\dagger_{j\sigma}c_{j\sigma}$ is the number operator, and $s_j^{+(-)} \equiv c^\dagger_{j\uparrow(\downarrow)} c_{j\downarrow(\uparrow)}$ the spin raising (lowering) operators. The t term mimics atomic motion via hopping. The U and J terms represent, respectively, the contact and nearest-neighbor parts of a same two-body interaction, from now on in $|t| = 1$ units.

We explore the quantum phases of the tUJ model by resorting to a DMRG method [38–40], as described in detail in the Supplemental Material [41], which includes Refs. [42–48]. We probe different quantum correlation functions $\langle O_i^\dagger O_j \rangle$, with O_k an operator acting on site k. We have considered spin density wave (SDW) correlations with $O = s^{x,y,z}$, charge density waves (CDW) with $O = n$, and superfluid pairing (SF) with $O = c_\uparrow c_\downarrow$. As we focus on the connection between the system quantum phases and their metrological usability, we only display results for $\nu = 1/4$ filling, though results at $\nu = 1/2$ are also discussed.

Quantum phases.—Figure 1 (bottom) displays the system quantum phases. We first discuss the phase diagram for $-\infty < U < +\infty$ and $|J|$ values below the solid thickest curves. Large and negative U favor a SF phase in the 1D sense with a large fraction of doubly occupied sites [49], while small J couplings are ineffective without opposite spins to pair. Moving towards $U \to 0$, on-site pairs progressively become disfavored, and hopping starts to dominate. As expected, this leads to CDW ordering for $J > 0$ and SDW^z for $J < 0, U > 0$, both characterized by a typical $2k_F$ oscillation in the correlation functions. Overall, the behavior around the origin is consistent with a smooth merging into a Luttinger-liquid (LL) description. Larger and positive U values drive instead a dominance of antiferromagnetic (AFM)-like ordering in the form of $\mathrm{SDW}^{x,y}$ oscillating correlation functions for $J > 0$. For $J < 0$, a positive and nonoscillatory power-law behavior sets in, along with suppression of the spin-z correlations, while the spin-x, y expectation values on each site are solid zeros. We call this the XY-ferromagnetic (XY-FM) phase in the 1D sense, the power-law decay being the longest range ordering possible [49]. All this suggests the many-body ground state to be fully symmetric in the xy pseudospin plane, as dictated by the symmetry of the Hamiltonian. The $\mathrm{SDW}^{x,y}$ and XY-FM phases can be understood noticing that $+J\sum_i (s_i^+ s_{i+1}^- + \mathrm{H.c.})$ can be cast as $\sim s_i^x s_{i+1}^x + s_i^y s_{i+1}^y$, so that spin-exchange coupling favors spin (anti-)alignment in the x, y plane.

We remark that a similar tUJ model has been investigated by Dziurzik *et al.* [35] in the context of high-temperature superconductivity via bosonization and DMRG techniques, exploring the J, U space at different fillings. While we find good agreement on the phases' nature and boundaries discussed so far (tilted dot-dashed lines in Fig. 1 [35]), our analysis provides qualitative and quantitative evidence of a new phase. In this phase, particles clusterize, i.e., form regions with unit density surrounded by zero density. Inside the clusters, spins are strongly aligned (FM) or antialigned (AFM) in their x, y components. In Fig. 1 these are the XY-FM and XY-AFM cluster phases, emerging for $J < 0$ and $J > 0$, respectively, above and below a U-dependent threshold J_c. We now investigate the nature of these phases, turning our attention to the density profiles displayed in Fig. 2 for the illustrative value $J/U = -0.1$ [41].

While for $U < 0$ and $U \lesssim 3$ values (top panel), the density profiles show the usual Friedel oscillations around average density [41], for $U \gtrsim 38$ we encounter the typical situation depicted in the lower panel. The system's bulk ceases to be translationally invariant, and fermions form clusters of singly occupied sites. Simultaneously, very strong spin-x correlations arise among particles inside clusters [41]. A similar simulation for the Hubbard model with $J = 0$ shows no trace of this phase (inset), leading us to infer that the cluster phase be driven by the dominance of the local nearest-neighbor (FM and AFM) xy coupling over the delocalizing hopping term. We assess the robustness of this phase by performing a number of runs against variations of simulation parameters. Though the clusters' positions and number are seen to change in a sensible manner, their qualitative behavior persists as detailed in

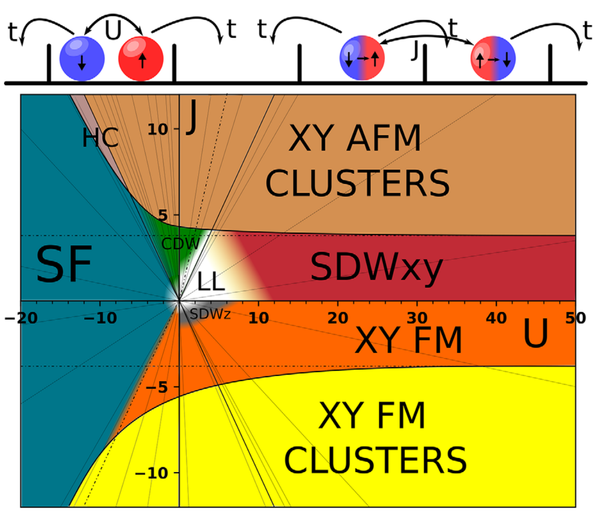

FIG. 1. System concept. Top. The tUJ Hamiltonian (1): t drives the hopping, U the on-site interaction, and J the spin-exchange coupling. Bottom. Qualitative phase diagram at quarter filling in the $U/t - J/t$ parameter space, including the following phases: Luttinger liquid, superfluid, charge-density-wave-like, spin-density wave, XY ferromagnetic, clusters with internal XY-FM or antiferromagnetic spin ordering, and *hemmed* clusters (see text for descriptions). Simulations have been performed along the solid lines. Thick solid straight lines: $|J/U| = 1$. Thick curves: Guidelines delimiting cluster phases. As $U \to +\infty$, $J_c \simeq 3.8$ separates AFM-like $\mathrm{SDW}^{x,y}$ and XY-AFM cluster phases, while $J_c \simeq -3.8$ separates XY-FM and XY-FM clusters. Dot-dashed straight lines: studies from Refs. [35] (tilted) and [37] (horizontal) (see text). We explore the metrological usability of these phases, finding XY-FM and XY-FM cluster phases especially convenient (see text).

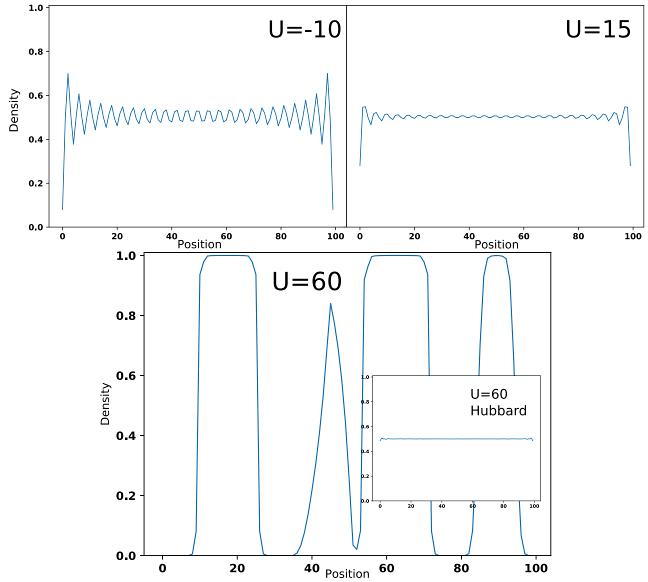

FIG. 2. Density profiles for $J = -0.1U$ and different U values. Top: typical profiles in the SF and CDW (left), SDW and XY-FM phases (right). Friedel oscillations are present [41]. Bottom: Density profile for $U = 60$ with cluster formation. Inset: same profile with $J = 0$.

Ref. [41]. In essence, with our DMRG algorithm, single clusters more likely form at relatively small system sizes ($L \lesssim 40$), and moving clusters may merge under larger numbers of finite-size algorithm iterations. We infer that the variability of the clusters' positions be due to the vanishing energetic cost of moving around one of them in the surrounding free space.

In fact, we found traces of this state in studies of the tJ model performed via exact diagonalization [37], yielding $J_c = 3.22$, and via DMRG, resulting in $J_c \simeq 3.15$ [50]. From our density profiles, we infer that the cluster phase appears at $U_c \simeq 38$, i.e.; given $J/U = -0.1$, $J_c \simeq -3.8$. We infer that this phase transition is driven by the same physical mechanism as in Ref. [37], but with a critical J_c modified by the on-site U. In fact, their no-double occupancy setting can be viewed as our $U \to +\infty$ limit, where we find $|J_c| \simeq 3.8$. For large $U < 0$, the boundary is instead located on the lines $|J/U| \sim \pm 0.85$. As one would expect $|J/U| = \pm 1$, the observed modified value could be due to superexchange. In the $-1 < J/U < -0.85$ gap, we observe peculiar clusters characterized by double occupancy at the density edges, which we name hemmed clusters (HC) [41]. This is not the case in the symmetric region with $J/U > 0$.

Quantum Fisher information.—Having characterized our quantum phases, we can now turn to measure their degree of many-body entanglement via quantum Fisher information F, and test the system's metrological usability. The quantum Cramér-Rao lower bound [14] on an estimator variance is given by $(\Delta\Theta)^2 = 1/F[\rho, \hat{S}]$. QFI depends in a complicated way on both the system's initial state and the transformation performed by the physical phenomenon to be measured, but it considerably simplifies for a pure state undergoing a unitary transformation $\exp(i\theta S_{\vec{a}})$, becoming $F[\psi, \hat{S}_{\vec{a}}] = 4(\Delta S_{\vec{a}})^2_\psi$ [14]. Here $S_{\vec{a}} \equiv a_\alpha S^\alpha$ is a linear combination of global (pseudo-)spin operators [14]. $F[\psi, \hat{S}_{\vec{a}}]$ fixes a criterion for evaluating the metrological usability of a quantum state, here the ground state of the many-fermion system. It is known that for an N-body uncorrelated product state, $F \sim N$ corresponds to the shot-noise limit [14]. For possibly good metrological usability then, QFI needs to scale as $N^\gamma <$, with $1 < \gamma < 2$ limited by the Heisenberg principle [13].

Results on QFI.—We now quantify these expectations by computing QFI across the phase diagram and comparing it with the quantum phases' order parameters. In all computations we select the spin axis that offers the largest QFI value from the angular momentum covariance matrix $\mathrm{Cov}_{ab} = \sum_{i,j}\langle s_i^a s_j^b\rangle$ [15], always obtaining the x axis as a nongranted outcome. A simple reasoning would lead us to infer that QFI on SDW or SF states would return a tiny value as compared even to shot-noise QFI $\sim N$. In fact, the oscillating spin-x correlations between different sites would add up to zero in the SDW and vanish for each doubly occupied site of the SF state. This view corresponds to our numerical findings. QFI results to be large only in the XY-FM and XY-FM cluster phases. For a quantitative comparison, we now define the corresponding order parameters. For the XY-FM phase, this is taken to be the area $CC_x(0)$ of the normalized $k = 0$ peak in the Fourier transform of the spin-x correlation function $C_x(i-j)$. For the clusters' phase, it is the normalized density variance $L^{-1}\sum_i(\Delta n^2)_i$.

Since we are originally interested in systems where J and U are effectively caused by the same term, we run simulations at fixed J/U while varying U to cross all possible phases. The results for QFI (red points and curve), XY-FM (green points and curve), and cluster (blue points and curve) order parameters are collected within one single graph in Fig. 3, one central result of the present work. We see that the QFI shows a steep change in correspondence of the quantum phase transition to spin-x ordering, the QFI and $CC_x(0)$ curves getting quite closely along with varying U. In fact, one may use QFI to infer the occurrence of the two quantum phase transitions around $U \sim 4$ and $U \sim 38$. The correspondence between QFI and order parameters is quantitative for the XY-FM phase. The fact that particles in different clusters are uncorrelated makes the comparison qualitative for the cluster phases at this stage. A quantitative treatment is recovered via the QFI scaling analysis below, generalizing this central message to different J/U values in the phase diagram. In particular, we now study the dependence of QFI on J/U and filling, and assess the degree of metrological usability from QFI scaling with the particle number $N = 2\nu L$ [51]. We display in Fig. 4 QFI

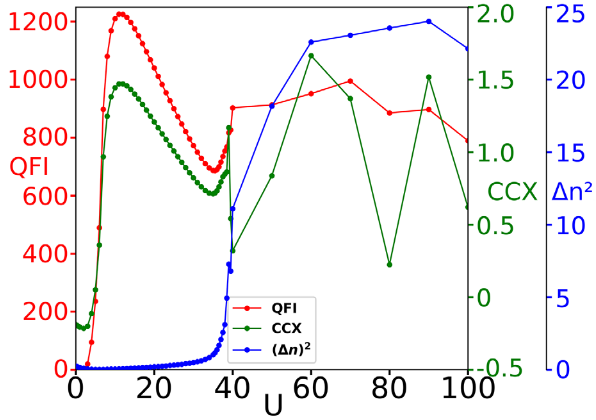

FIG. 3. Quantum fermionic correlated phases and metrological usability in a single-shot phase diagram. The QFI (red) vs U gets along the order parameters $CC_x(0)$ (green) and $\sum_i(\Delta n^2)_i$ (blue) describing the building up of XY-FM and cluster correlations, respectively (see text).

density QFI/N at two commensurate fillings, $1/4$ (red) and $1/2$ (blue). As anticipated, QFI vanishes for $U < 0$ and $J/U = +0.8$, where XY-FM and cluster phases are absent. At $\nu = 1/2$, QFI density is larger and, unlike $\nu = 1/4$, smooth since the whole system is in the form of a single cluster. For both fillings, larger (negative) values of J favor cluster formation and steeper QFI rise.

We study the N scaling with special care at $\nu = 1/4$, where several uncorrelated clusters may form at large $U > 0$. Thus, we keep relatively small system sizes ($L < 40$) to have one single cluster [41]. For both fillings, we fit the QFI dependence on N with QFI $= kN^\gamma$, as

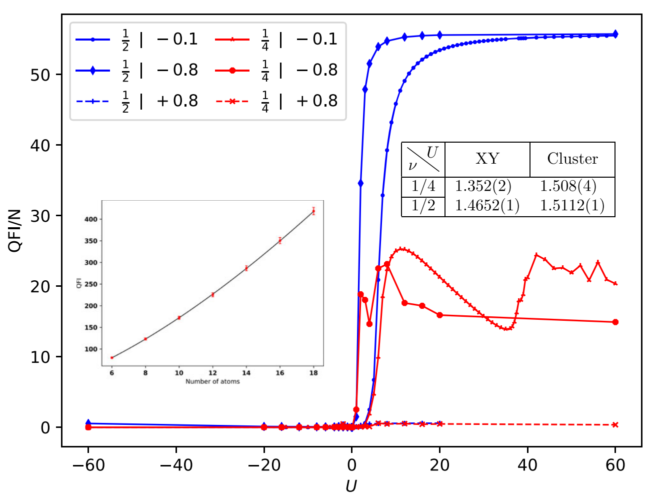

FIG. 4. QFI density QFI/N (N number of atoms) vs U for $\nu = 1/4$ (red) and $1/2$ (blue), and different J/U (see legend). Table: exponents fitted from QFI $= kN^\gamma$ for $\nu = 1/2$, $1/4$ at $J/U = -0.1$. U values are chosen to correspond to the QFI maximum in the XY-FM phase ($U = 11$) and in the large-U limit for the cluster phase ($U = 60$), at $\nu = 1/4$. Inset figure: example of QFI scaling for $\nu = 1/4$, $U = 60$, and $J/U = -0.1$.

illustrated in the inset. The table in Fig. 4 reports γ for $U = 11$, corresponding to the QFI maximum in the XY-FM phase, and the large-U limit for the cluster phase at $\nu = 1/4$. We see that half-filling shows better scaling outside the cluster region. Inside it, the scalings at $\nu = 1/4$ and $1/2$ are compatible within error.

Metrology implementations.—QFI scaling is promising, but a real use of these reduced-quantum uncertainty states injected in an interferometric sequence requires suited protocols. The XY-FM and cluster phases represent non-Gaussian states with a Wigner distribution located around the equator in the Bloch sphere [41] and $\langle S_{x,y,z}\rangle = 0$, so that the signal cannot be encoded in a mean spin direction. This unconventional situation reminds us of the one experimentally investigated in Ref. [52] for twin-Fock states with the method proposed in Ref. [53]. Adopting a similar strategy, one might operate a rotation by angle θ about an axis in the xy plane, and consider the lower bound $\mathcal{F} \geq |d\langle S_z^2\rangle/d\theta|^2/(\Delta S_z^2)^2$ for the classical Fisher information, leading to the uncertainty $\Delta\theta \geq (\sqrt{\mathcal{F}n})$ after n measurements. In essence, the signal would be related to the second moment of S_z instead of the first one, and the noise to the fourth instead of the second. Eventually, optimization with respect to θ is to be performed. Signal extraction and optimization can be operated after sampling the full probability distribution or the second and fourth S_z momenta [54] in a time-dependent simulation of the interferometric sequence.

Conclusions.—Our study conveys two unforeseen messages. First, short-range interactions are able to build metrologically useful entanglement in a many-fermion system. This is demonstrated by a large degree of quantum Fisher information, accompanied by interesting scaling with the number of particles. The best performing phase is indeed the cluster one, driven by the J coupling, which in our study models the short-range interactions. Second, our results imply that QFI represents a powerful tool to characterize the phases of the quantum fluid, acting as an order parameter.

Implementations in ultracold gases platforms may include currently realized systems of dipolar fermions in optical lattices [55] and suitably engineered versions of Fermi-Hubbard setups [56] in both cases after further reduction of dimensionality to one dimension. Finally, a microscopic origin of this tUJ model can be provided by a photon-mediated effective interaction among fermions in an optical cavity [57], leading to a spin-squeezing-like Hamiltonian [15]. Multimode optical cavities [58] may bring in the short-range environment, though a realistic probe requires detailed modeling to include unavoidable dissipation processes [59]. Single-particle decoherence could be suppressed in the presence of a spin gap, as in the cluster phase [35]. While one might expect superradiance-enhanced decoherence to still be an issue, one might ask whether delocalization in Eq. (1) and the xy-symmetric structure of the ground state might be exploited to limit the effect. We are currently working along this direction, via an actual time-dependent simulation of the open system [59].

We thank Davide Rossini for valuable support in using his DMRG code. We are grateful to Augusto Smerzi for enlightening discussions on actual protocols. We thank Luca Lepori and Luca Pezzè for useful discussions, and Benjamin Lev, Jonathan Keeling, and Andrew Daley for collaborative work on optical-cavities implementations. M. L. C. thanks JILA for fruitful and warm hospitality during the visiting fellowship, when part of this work has been carried out, and in particular Ana Maria Rey and Murray Holland for enriching discussions. M. L. C. would like to thank KITP for hospitality during the program on Open Quantum Systems, when discussions have revealed to be useful also to envisage possible follow-ups of this work. This research was supported in part by the National Science Foundation under Grant No. NSF PHY-1748958. We acknowledge the MAGIA-Advanced project for support and the Goldrake HPC team.

*Corresponding author.
maria.luisa.chiofalo@unipi.it

[1] L. Pezzè, A. Smerzi, M. K. Oberthaler, R. Schmied, and P. Treutlein, Quantum metrology with nonclassical states of atomic ensembles, Rev. Mod. Phys. **90**, 035005 (2018).
[2] J. Ye, H. J. Kimble, and H. Katori, Quantum State Engineering and Precision Metrology Using State-Insensitive Light Traps, Science **320**, 1734 (2008).
[3] V. Giovannetti, S. Lloyd, and L. Maccone, Advances in quantum metrology, Nat. Photonics **5**, 222 (2011).
[4] K. Molmer and A. Sorensen, Multiparticle Entanglement of Hot Trapped Ions, Phys. Rev. Lett. **82**, 1835 (1999).
[5] M. A. Kasevich, Coherence with Atoms, Science **298**, 1363 (2002).
[6] *Atom Interferometry, Proc. Intl. School "E. Fermi"*, edited by G. Tino and M. A. Kasevich (IOS Press, Amsterdam and Bologna, 2013).
[7] A. D. Cronin, J. Schmiedmayer, and D. E. Pritchard, Optics and interferometry with atoms and molecules, Rev. Mod. Phys. **81**, 1051 (2009).
[8] M. Kasevich and S. Chu, Atomic Interferometry Using Stimulated Raman Transitions, Phys. Rev. Lett. **67**, 181 (1991).
[9] H. Müller, A. Peters, and S. Chu, A precision measurement of the gravitational redshift by the interference of matter waves, Nature (London) **463**, 926 (2010).
[10] G. Rosi, F. Sorrentino, L. Cacciapuoti, M. Prevedelli, and G. M. Tino, Precision measurement of the Newtonian gravitational constant using cold atoms, Nature (London) **510**, 518 (2014).
[11] V. V. Ivanov, A. Alberti, M. Schioppo, G. Ferrari, M. Artoni, M. L. Chiofalo, and G. M. Tino, Coherent Delocalization of Atomic Wave Packets in Driven Lattice Potentials, Phys. Rev. Lett. **100**, 043602 (2008).
[12] P. W. Graham, J. M. Hogan, M. A. Kasevich, and S. Rajendran, New Method for Gravitational Wave Detection with Atomic Sensors, Phys. Rev. Lett. **110**, 171102 (2013).
[13] V. Giovannetti, S. Lloyd, and L. Maccone, Quantum Metrology, Phys. Rev. Lett. **96**, 010401 (2006).
[14] L. Pezzè and A. Smerzi, Quantum theory of phase estimation, in Ref. [6], p. 691.
[15] J. Ma, X. Wang, C. Sun, and F. Nori, Quantum spin squeezing, Phys. Rep. **509**, 89 (2011).
[16] C. Gross, T. Zibold, E. Nicklas, J. Estève, and M. K. Oberthaler, Nonlinear atom interferometer surpasses classical precision limit, Nature (London) **464**, 1165 (2010).
[17] H. P. Robertson, The uncertainty principle, Phys. Rev. **34**, 163 (1929).
[18] M. Kitagawa and M. Ueda, Squeezed spin states, Phys. Rev. A **47**, 5138 (1993).
[19] D. F. Walls, Squeezed states of light, Nature (London) **306**, 141 (1983).
[20] I. D. Leroux, M. H. Schleier-Smith, and V. Vuletić, Implementation of Cavity Squeezing of a Collective Atomic Spin, Phys. Rev. Lett. **104**, 073602 (2010).
[21] J. G. Bohnet, K. C. Cox, M. A. Norcia, J. M. Weiner, Z. Chen, and J. K. Thompson, Reduced spin measurement back-action for a phase sensitivity ten times beyond the standard quantum limit, Nat. Photonics **8**, 731 (2014).
[22] M. A. Norcia, R. J. Lewis-Swan, J. R. K. Cline, B. Zhu, A. M. Rey, and J. K. Thompson, Cavity-mediated collective spin-exchange interactions in a strontium superradiant laser, Science **361**, 259 (2018).
[23] H. Ritsch, P. Domokos, F. Brennecke, and T. Esslinger, Cold atoms in cavity-generated dynamical optical potentials, Rev. Mod. Phys. **85**, 553 (2013).
[24] P. Hyllus, W. Laskowski, R. Krischek, C. Schwemmer, W. Wieczorek, H. Weinfurter, L. Pezzé, and A. Smerzi, Fisher information and multiparticle entanglement, Phys. Rev. A **85**, 022321 (2012).
[25] M. Gabbrielli, L. Lepori, and L. Pezzè, Multipartite-entanglement tomography of a quantum simulator, New J. Phys. **21**, 033039 (2019).
[26] A. S. Buyskikh, M. Fagotti, J. Schachenmayer, F. Essler, and A. J. Daley, Entanglement growth and correlation spreading with variable-range interactions in spin and fermionic tunneling models, Phys. Rev. A **93**, 053620 (2016).
[27] M. Foss-Feig, Z. Gong, A. Gorshkov, and C. Clark, Entanglement and spin-squeezing without infinite-range interactions, arXiv:1612.07805.
[28] K. Eckert, J. Schliemann, D. Bruß, and M. Lewenstein, Quantum correlations in systems of indistinguishable particles, Ann. Phys. (Amsterdam) **299**, 88 (2002).
[29] P. Zanardi, Quantum entanglement in fermionic lattices, Phys. Rev. A **65**, 042101 (2002).
[30] R. Lo Franco and G. Compagno, Quantum entanglement of identical particles by standard information-theoretic notions, Sci. Rep. **6**, 20603 (2016).
[31] A. C. Lourenço, T. Debarba, and E. I. Duzzioni, Entanglement of indistinguishable particles: A comparative study, Phys. Rev. A **99**, 012341 (2019).
[32] P. Hauke, M. Heyl, L. Tagliacozzo, and P. Zoller, Measuring multipartite entanglement through dynamic susceptibilities, Nat. Photonics **12**, 778 (2016).

[33] A. M. Kaufman, B. J. Lester, M. Foss-Feig, M. L. Wall, A. M. Rey, and C. A. Regal, Entangling two transportable neutral atoms via local spin exchange, Nature (London) **527**, 208 (2015).

[34] L. Salvi, N. Poli, V. Vuletić, and G. M. Tino, Squeezing on Momentum States for Atom Interferometry, Phys. Rev. Lett. **120**, 033601 (2018).

[35] C. Dziurzik, G. I. Japaridze, A. Schadschneider, I. Titvinidze, and J. Zittartz, Triplet superconductivity in a 1D itinerant electron system with transverse spin anisotropy, Eur. Phys. J. B **51**, 41 (2006).

[36] S. P. Nolan, S. S. Szigeti, and S. A. Haine, Optimal and Robust Quantum Metrology Using Interaction-Based Readouts, Phys. Rev. Lett. **119**, 193601 (2017).

[37] M. Ogata, M. U. Luchini, S. Sorella, and F. F. Assaad, Phase diagram of the one-dimensional t-J model, Phys. Rev. Lett. **66**, 2388 (1991).

[38] S. R. White, Density Matrix Formulation for Quantum Renormalization Groups, Phys. Rev. Lett. **69**, 2863 (1992).

[39] U. Schollwöck, The density-matrix renormalization group, Rev. Mod. Phys. **77**, 259 (2005).

[40] G. De Chiara, M. Rizzi, D. Rossini, and S. Montangero, Density matrix renormalization group for dummies, J. Comput. Theor. Nanosci. **5**, 1277 (2008).

[41] See Supplemental Material at http://link.aps.org/supplemental/10.1103/PhysRevLett.123.060406 contains additional information and details on the DMRG method and algorithm, the quantum Fisher information, the relevant correlation functions across the whole phase diagram, especially in the cluster phase, and on the metrology implementations.

[42] O. Legeza and G. Fáth, Accuracy of the density-matrix renormalization-group method, Phys. Rev. B **53**, 14349 (1996).

[43] M. Andersson, M. Boman, and S. Östlund, Density-matrix renormalization group for a gapless system of free fermions, Phys. Rev. B **59**, 10493 (1999).

[44] G. Bedürftig, B. Brendel, H. Frahm, and R. M. Noack, Friedel oscillations in the open Hubbard chain, Phys. Rev. B **58**, 10225 (1998).

[45] O. E. Barndorff-Nielsen and R. D. Gill, Fisher information in quantum statistics, J. Phys. A **33**, 4481 (2000).

[46] T. Macrì, A. Smerzi, and L. Pezzè, Loschmidt echo for quantum metrology, Phys. Rev. A **94**, 010102(R) (2016).

[47] D. J. Wineland, J. J. Bollinger, W. M. Itano, F. L. Moore, and D. J. Heinzen, Spin squeezing and reduced quantum noise in spectroscopy, Phys. Rev. A **46**, R6797 (1992).

[48] G. I. Japaridze and E. Müller-Hartmann, Triplet superconductivity in a one-dimensional ferromagnetic t-J model, Phys. Rev. B **61**, 9019 (2000).

[49] T. Giamarchi, *Quantum Physics in One Dimension*, Int. Ser. Monogr. Phys. (Clarendon Press, Oxford, 2003).

[50] A. Moreno, A. Muramatsu, and S. R. Manmana, Ground-state phase diagram of the one-dimensional t-J model, Phys. Rev. B **83**, 205113 (2011).

[51] L. Pezzé and A. Smerzi, Entanglement, Nonlinear Dynamics, and the Heisenberg Limit, Phys. Rev. Lett. **102**, 100401 (2009).

[52] B. Lücke, M. Scherer, J. Kruse, L. Pezzé, F. Deuretzbacher, P. Hyllus, O. Topic, J. Peise, W. Ertmer, J. Arlt *et al.*, Twin Matter Waves for Interferometry Beyond the Classical Limit, Science **334**, 773 (2011).

[53] T. Kim, O. Pfister, M. J. Holland, J. Noh, and J. L. Hall, Influence of decorrelation on Heisenberg-limited interferometry with quantum correlated photons, Phys. Rev. A **57**, 4004 (1998).

[54] H. Strobel, W. Muessel, D. Linnemann, T. Zibold, D. B. Hume, L. Pezzè, A. Smerzi, and M. K. Oberthaler, Fisher information and entanglement of non-Gaussian spin states, Science **345**, 424 (2014).

[55] S. Baier, D. Petter, J. H. Becher, A. Patscheider, G. Natale, L. Chomaz, M. J. Mark, and F. Ferlaino, Realization of a Strongly Interacting Fermi Gas of Dipolar Atoms, Phys. Rev. Lett. **121**, 093602 (2018).

[56] A. Mazurenko, C. S. Chiu, G. Ji, M. F. Parsons, M. Kanász-Nagy, R. Schmidt, F. Grusdt, E. Demler, D. Greif, and M. Greiner, A cold-atom Fermi-Hubbard antiferromagnet, Nature (London) **545**, 462 (2017).

[57] E. Colella, R. Citro, M. Barsanti, D. Rossini, and M.-L. Chiofalo, Quantum phases of spinful Fermi gases in optical cavities, Phys. Rev. B **97**, 134502 (2018).

[58] V. D. Vaidya, Y. Guo, R. M. Kroeze, K. E. Ballantine, A. J. Kollár, J. Keeling, and B. L. Lev, Tunable-Range, Photon-Mediated Atomic Interactions in Multimode Cavity QED, Phys. Rev. X **8**, 011002 (2018).

[59] J. Keeling, B. Lev, and A. Daley (private communication).